Spinal Endocannabinoids and CB1 Receptors Mediate C-Fiber Induced Heterosynaptic Pain Sensitization

Alejandro J. Pernía-Andrade, *et al.*

Science **325**, 760 (2009);
DOI: 10.1126/science.1171870

4.25 ±1.9 pA of NMDA current at resting membrane potential. In addition, we measured directly (830 to 950 μm from the soma) the total and NMDA just-suprathreshold current needed for NMDA spike initiation using glutamate uncaging (total current of 187 ± 43 pA; NMDA current of 88 ± 19 pA; $n = 5$) (fig. S2D). Using these parameters, NMDA spikes could be initiated at all locations on the tuft tree; however, the number of synapses needed was far lower in the very distal tuft branches. Just 8.75 ± 2.21 synapses were needed to evoke NMDA spikes near the ends of the tuft branches, whereas up to 43 ± 4.54 synapses were needed at 250 μm from the pia, leading to a depolarization of 1.07 ± 0.25 mV and 9.22 ± 1.4 mV, respectively, at the calcium spike initiation zone (fig. S2). The contribution of voltage-gated calcium channels was negligible at the tuft regions (fig. S2) but became prominent at the apical calcium initiation zone (extending ~340 μm from the first bifurcation), where a full-blown calcium spike was evoked (fig. S2).

When we activated randomly distributed synapses at the tuft dendrites, which usually leads to NMDA spike initiation at multiple branches, we found that 116.66 ± 25.59 randomly distributed synapses (2.9% of total synapses) over the whole tuft region are sufficient to trigger a calcium spike (Fig. 4F). Interestingly, when we redistributed the activated synapses based on bifurcation order, calcium spikes were most readily initiated by third- and fourth-order branches (100.83 ± 11.64 and 99 ± 28.75 synapses, respectively) (Fig. 4F). Blocking NMDA receptors caused a dramatic increase in the number of synapses at tuft branches needed for calcium spike initiation. In this scenario, the number of synapses increased exponentially with branch order, from 408.33 ± 59.69 synapses near the main bifurcation to 5550 ± 4749 synapses at the terminal branches (exceeding the total spine number at these dendrites) (*33*) (Fig. 4F). In contrast, NMDA spikes only modestly contributed to the initiation of calcium spikes when synapses were activated at the calcium initiation zone itself (Fig. 4F, first bifurcation). On the other hand, uniformly increasing calcium conductance in tuft branches (up to a factor of 3) did not change the requirement for an exponential increase in the number of pure AMPA synapses needed to initiate a calcium spike at the main bifurcation point.

Thus, there are three stages (thresholds) in the integration of top-down associative information terminating at distal tuft branches: (i) NMDA spike initiation at the distal tuft branches, (ii) Ca^{2+} spike initiation near the main bifurcation, and (iii) sodium spike initiation at the axon hillock (Fig. 4, G and H).

Taking all the properties together, a new unifying principle emerges as to how pyramidal neurons integrate synaptic information. The thin distal tuft and basal dendrites of pyramidal neurons, which receive the overwhelming majority of synaptic inputs (*33*), appear to constitute a class of dendrite in which NMDA spikes are the predominant regenerative events summing synaptic inputs in semi-independent compartments. The output of each subunit in this class of dendrite is passed on to the major sites of integration at the axon and apical calcium initiation zones, which can all interact via actively propagated signals (*34*), enabling the interactions between top-down and bottom-up information.

References and Notes

1. D. J. Felleman, D. C. Van Essen, *Cereb. Cortex* **1**, 1 (1991).
2. K. S. Rockland, D. N. Pandya, *Brain Res.* **179**, 3 (1979).
3. J. M. Budd, *Proc. R. Soc. London Ser. B Biol. Sci.* **265**, 1037 (1998).
4. B. Kuhn, W. Denk, R. M. Bruno, *Proc. Natl. Acad. Sci. U.S.A.* **105**, 7588 (2008).
5. L. Petreanu, T. Mao, S. M. Sternson, K. Svoboda, *Nature* **457**, 1142 (2009).
6. P. Rubio-Garrido, F. Pérez-de-Manzo, C. Porrero, M. J. Galazo, F. Clascá, *Cereb. Cortex*; published online 2 February 2009 (10.1093/cercor/bhn259).
7. O. Bernander, C. Koch, R. J. Douglas, *J. Neurophysiol.* **72**, 2743 (1994).
8. M. Häusser, N. Spruston, G. J. Stuart, *Science* **290**, 739 (2000).
9. N. Spruston, *Nat. Rev. Neurosci.* **9**, 206 (2008).
10. T. Nevian, M. E. Larkum, A. Polsky, J. Schiller, *Nat. Neurosci.* **10**, 206 (2007).
11. J. Schiller, G. Major, H. J. Koester, Y. Schiller, *Nature* **404**, 285 (2000).
12. B. A. Milojkovic, J. P. Wuskell, L. M. Loew, S. D. Antic, *J. Membr. Biol.* **208**, 155 (2005).
13. H. G. Kim, B. W. Connors, *J. Neurosci.* **13**, 5301 (1993).
14. J. Schiller, Y. Schiller, G. Stuart, B. Sakmann, *J. Physiol. London* **505**, 605 (1997).
15. M. E. Larkum, K. M. Kaiser, B. Sakmann, *Proc. Natl. Acad. Sci. U.S.A.* **96**, 14600 (1999).
16. M. E. Larkum, J. J. Zhu, B. Sakmann, *Nature* **398**, 338 (1999).
17. A. Polsky, B. W. Mel, J. Schiller, *Nat. Neurosci.* **7**, 621 (2004).
18. R. Yuste, M. J. Gutnick, D. Saar, K. R. Delaney, D. W. Tank, *Neuron* **13**, 23 (1994).
19. M. E. Larkum, J. J. Zhu, *J. Neurosci.* **22**, 6991 (2002).
20. P. A. Rhodes, R. R. Llinás, *J. Physiol.* **536**, 167 (2001).
21. S. R. Williams, G. J. Stuart, *Trends Neurosci.* **26**, 147 (2003).
22. J. Bullier, *Brain Res. Brain Res. Rev.* **36**, 96 (2001).
23. The dendritic spike was probably larger than this at the site of initiation, which was most likely closer to the stimulating electrode.
24. Distal dendritic recording sites were chosen on the basis of dendritic thickness and the lack of Ca^{2+} spike initiation.
25. T. Berger, M. E. Larkum, H. R. Lüscher, *J. Neurophysiol.* **85**, 855 (2001).
26. S. R. Williams, G. J. Stuart, *J. Neurophysiol.* **83**, 3177 (2000).
27. A. Lörincz, T. Notomi, G. Tamás, R. Shigemoto, Z. Nusser, *Nat. Neurosci.* **5**, 1185 (2002).
28. P. A. Rhodes, in *Cerebral Cortex, Vol. 13*, P. S. Ulinski, E. G. Jones, A. Peters, Eds. (Plenum, New York, 1999), pp. 139–200.
29. C. Koch, I. Segev, *Nat. Neurosci.* **3** (suppl.), 1171 (2000).
30. N. Spruston, W. L. Kath, *Nat. Neurosci.* **7**, 567 (2004).
31. M. London, M. Häusser, *Annu. Rev. Neurosci.* **28**, 503 (2005).
32. With the I_h-blocker ZD7288, single NMDA spikes sometimes caused Ca^{2+} spikes.
33. A. U. Larkman, *J. Comp. Neurol.* **306**, 332 (1991).
34. M. E. Larkum, J. J. Zhu, B. Sakmann, *J. Physiol. London* **533**, 447 (2001).

35. We thank B. Sakmann for generous support and comments on the manuscript and Y. Schiller for helpful comments and discussions on the manuscript. We thank K. Fischer for Neurolucida reconstructions of the biocytin-filled neurons. This study was supported by NIH, the Israel Science Foundation, and the Rappaport Foundation (J.S.); by the Swiss National Science Foundation (M.L., grant PP0033-119159; T.N., grant 3100A0-118395); and by SystemsX.ch (M.L., Neurochoice). The authors declare that they have no competing financial interests.

Supporting Online Material

www.sciencemag.org/cgi/content/full/325/5941/756/DC1
Materials and Methods
Figs. S1 to S4
References

6 February 2009; accepted 24 June 2009
10.1126/science.1171958

Spinal Endocannabinoids and CB_1 Receptors Mediate C-Fiber–Induced Heterosynaptic Pain Sensitization

Alejandro J. Pernía-Andrade,[1]*† Ako Kato,[1,9]* Robert Witschi,[1,9]* Rita Nyilas,[2] István Katona,[2] Tamás F. Freund,[2] Masahiko Watanabe,[3] Jörg Filitz,[4] Wolfgang Koppert,[4]‡ Jürgen Schüttler,[4] Guangchen Ji,[5] Volker Neugebauer,[5] Giovanni Marsicano,[6] Beat Lutz,[7] Horacio Vanegas,[8] Hanns Ulrich Zeilhofer[1,9]§

Diminished synaptic inhibition in the spinal dorsal horn is a major contributor to chronic pain. Pathways that reduce synaptic inhibition in inflammatory and neuropathic pain states have been identified, but central hyperalgesia and diminished dorsal horn synaptic inhibition also occur in the absence of inflammation or neuropathy, solely triggered by intense nociceptive (C-fiber) input to the spinal dorsal horn. We found that endocannabinoids, produced upon strong nociceptive stimulation, activated type 1 cannabinoid (CB_1) receptors on inhibitory dorsal horn neurons to reduce the synaptic release of γ-aminobutyric acid and glycine and thus rendered nociceptive neurons excitable by nonpainful stimuli. Our results suggest that spinal endocannabinoids and CB_1 receptors on inhibitory dorsal horn interneurons act as mediators of heterosynaptic pain sensitization and play an unexpected role in dorsal horn pain-controlling circuits.

Activity-dependent central hyperalgesia can be induced in the absence of any inflammation or nerve damage by selective activation of glutamatergic C-fiber nociceptors; for example, with the specific transient receptor potential channel (TRP) V1 agonist capsaicin. Local subcutaneous injection of capsaicin induces primary hyperalgesia at the site of injection and a purely mechanical secondary hyperalgesia in the surrounding healthy skin (*1*). This secondary hyperalgesia originates from changes in the central processing of input from mechano-

sensitive A fibers and is characterized by an exaggerated sensitivity to painful stimuli and by pain evoked by light tactile stimulation (allodynia or touch-evoked pain). These symptoms are mimicked by the blockade of inhibitory γ-aminobutyric acid–mediated (GABAergic) and glycinergic neurotransmission in the spinal dorsal horn (*2*, *3*), suggesting that a loss of synaptic inhibition also accounts for C-fiber–induced secondary hyperalgesia. Activity-dependent hyperalgesia can thus be regarded as a correlate of heterosynaptic depression of inhibition (*4*). In many neuronal circuits of the central nervous system, endocannabinoids [2-arachidonoyl glycerol (2-AG) and anandamide (AEA)] are released upon intense activation of metabotropic glutamate receptors and serve as retrograde messengers mediating either homosynaptic feedback inhibition or heterosynaptic depression of (GABAergic) inhibition (*5*, *6*). Type 1 cannabinoid (CB_1) receptors are densely expressed in the superficial dorsal horn of the spinal cord (*7*), where they exert anti-hyperalgesia in different inflammatory or neuropathic disease states (*8*, *9*).

To define the role of CB_1 receptors in dorsal horn neuronal circuits, we first characterized the effects of CB_1 receptor activation on neurotransmission in mouse transverse spinal cord slices (Fig. 1). Excitatory and inhibitory postsynaptic currents (EPSCs and IPSCs) were evoked by extracellular electrical field stimulation at a frequency of four per minute and recorded from visually identified neurons in the superficial spinal dorsal horn (laminae I and II) (*10*). The mixed CB_1/CB_2 receptor agonist WIN 55,212-2 (3 μM) reversibly reduced the amplitudes of glycine receptor IPSCs to 64.3 ± 3.5% of control amplitudes (mean ± SEM, $n = 13$ neurons, $P < 0.001$, paired Student's t test) (Fig. 1A). Similarly, $GABA_A$ receptor IPSCs were reduced to 64.7 ± 3.0% ($P < 0.001$, $n = 8$ neurons, paired Student's t test) (Fig. 1B). The inhibition of IPSCs by WIN 55,212-2 was confined to the superficial dorsal horn, reversed by the CB_1 receptor antagonist/inverse agonist AM 251 (5 μM) (Fig. 1, A and B), and absent in global CB_1 receptor–deficient mice ($CB_1^{-/-}$ mice) (*11*) and in mice lacking CB_1 receptors specifically in dorsal horn inhibitory interneurons (*ptf1a*-$CB_1^{-/-}$ mice) (*12*) (fig. S1). WIN 55,212-2 had virtually no effect on EPSCs mediated by glutamate receptors of the α-amino-3-hydroxy-5-methylisoxazole (AMPA) subtype (AMPA-EPSCs) [Fig. 1C, see also (*13*)]. It did, however, reduce the amplitudes of monosynaptic AMPA-EPSCs evoked by stimulation of dorsal root primary afferent nerve fibers at C-fiber intensity by 34.5 ± 3.3% ($n = 9$ neurons). This inhibition was not reversed by AM 251 (fig. S2). We next tested whether stimulation of endogenous endocannabinoid production through the activation of group I metabotropic glutamate receptors (mGluR1/5) would have a similar effect on inhibitory synaptic transmission. These experiments were carried out in GlyT2–enhanced green fluorescent protein (GlyT2-EGFP) transgenic mice, which allowed targeted recordings from glycinergic (EGFP-positive) and nonglycinergic (EGFP-negative), presumed excitatory, interneurons (*14*). (*S*)-3,5-dihydroxyphenylglycine (DHPG, 10 μM), an agonist at mGluR1/5, reduced IPSC amplitudes in nonglycinergic presumed excitatory superficial dorsal horn neurons by 40.6 ± 4.5% ($n = 8$ neurons) (Fig. 1D). This inhibition was reversed by AM 251 (5 μM) (Fig. 1D) and partially prevented by mGluR1 and mGluR5 antagonists (LY

[1]Institute of Pharmacology and Toxicology, University of Zurich, Winterthurerstrasse 190, CH-8057 Zurich, Switzerland. [2]Institute of Experimental Medicine, Hungarian Academy of Sciences, H-1083 Budapest, Hungary. [3]Department of Anatomy, Hokkaido University School of Medicine, Sapporo 060-8638, Japan. [4]Department of Anesthesiology, University of Erlangen-Nürnberg, Krankenhausstrasse 12, D-91054 Erlangen, Germany. [5]Department of Neuroscience and Cell Biology, University of Texas Medical Branch, Galveston, TX 77555–1069, USA. [6]U862 Centre de Recherche INSERM François Magendie, 33077 Bordeaux, France. [7]Institute of Physiological Chemistry and Pathobiochemistry, Johannes Gutenberg-University Mainz, D-55099 Mainz, Germany. [8]Instituto Venezolano de Investigaciones Cientificas, Apartado 20632, Caracas 1020A, Venezuela. [9]Institute of Pharmaceutical Sciences, ETH Zurich, Wolfgang Pauli Strasse 10, CH-8093 Zurich, Switzerland.

*These authors contributed equally to this work.
†Present address: Institute of Physiology, University of Freiburg, Engesserstrasse 4, D-79108, Freiburg, Germany.
‡Present address: Department of Anesthesiology, Medical School Hannover, D-30625 Hannover, Germany.
§To whom correspondence should be addressed. E-mail: zeilhofer@pharma.uzh.ch

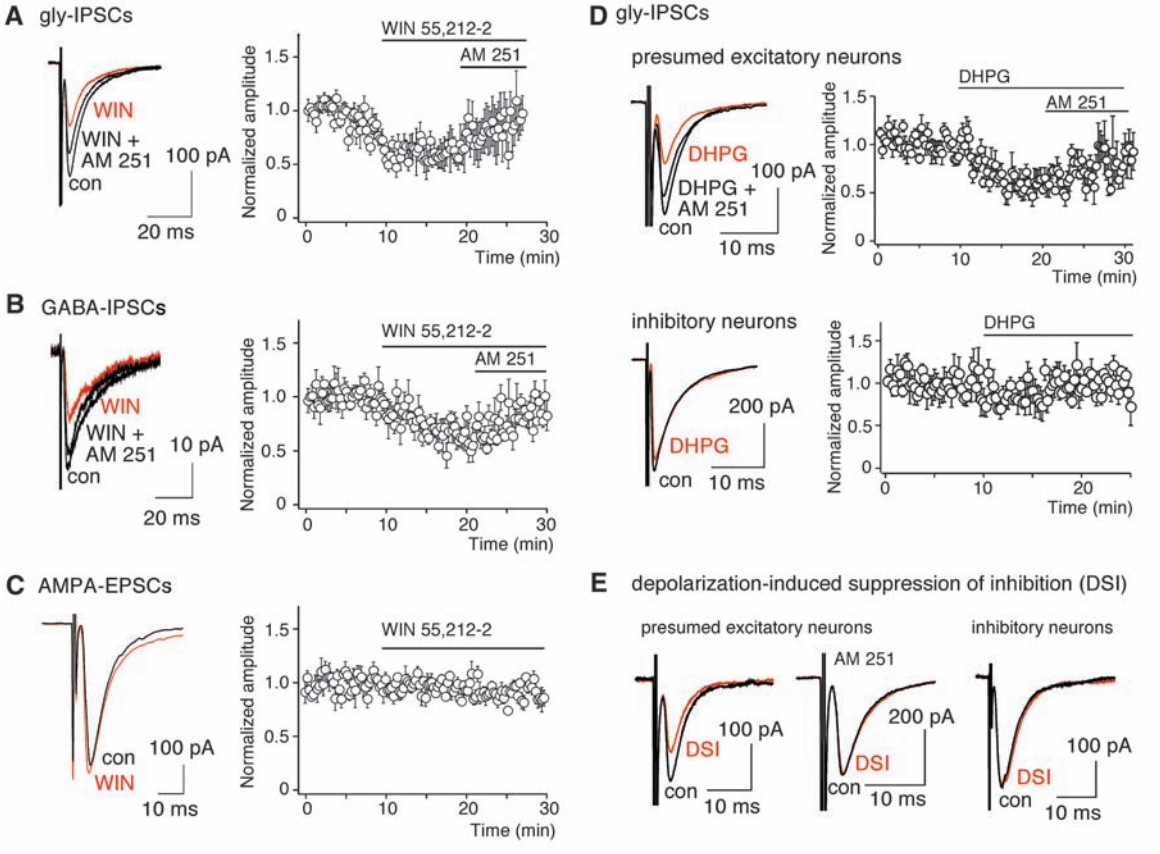

Fig. 1. Synaptic effects of CB_1 receptor activation in dorsal horn neuronal circuits. (**A** to **C**) Effects of the mixed CB_1/CB_2 receptor agonist WIN 55,212-2 (3 μM) on glycinergic IPSCs (A), GABAergic IPSCs (B), and AMPA-EPSCs (C). Left panels: Current traces averaged from 10 consecutive stimulations under control conditions, after addition of WIN 55,212-2 and after the additional application of AM 251 (5 μM). Right panels: Time course. Mean ± SEM, n = 7 to 13 neurons. (**D**) Inhibition of glycinergic IPSCs in nonglycinergic (EGFP-negative) neurons ($n = 8$ neurons) by the mGluR1/5 agonist DHPG (10 μM) and its reversal by AM 251 (5 μM). Only a minor inhibition was observed in glycinergic (EGFP-positive) neurons ($n = 8$ neurons). (**E**) DSI (1-s depolarization of the postsynaptic neuron to 0 mV) in nonglycinergic neurons (six out of eight neurons) and its prevention by AM 251 (5 μM). No DSI occurred in glycinergic neurons ($n = 5$ neurons). Glycinergic IPSCs were evoked at a frequency of 0.2 Hz.

367,385, 100 μM, remaining inhibition 21.0 ± 3.9%, n = 5 neurons; and MPEP, 10 μM, 25.0 ± 3.4%, n = 5 neurons) (fig. S3). Glycinergic input to EGFP-positive (glycinergic) neurons was less sensitive to DHPG, with an average reduction of only 10.3 ± 3.6% (n = 8 neurons) (Fig. 1D). Depolarization-induced suppression of inhibition (DSI) could be induced in six out of eight non-glycinergic neurons but was not seen in glycinergic neurons (n = 5 neurons) (Fig. 1E).

The reduction of inhibitory synaptic transmission by endocannabinoids was due to dimin-

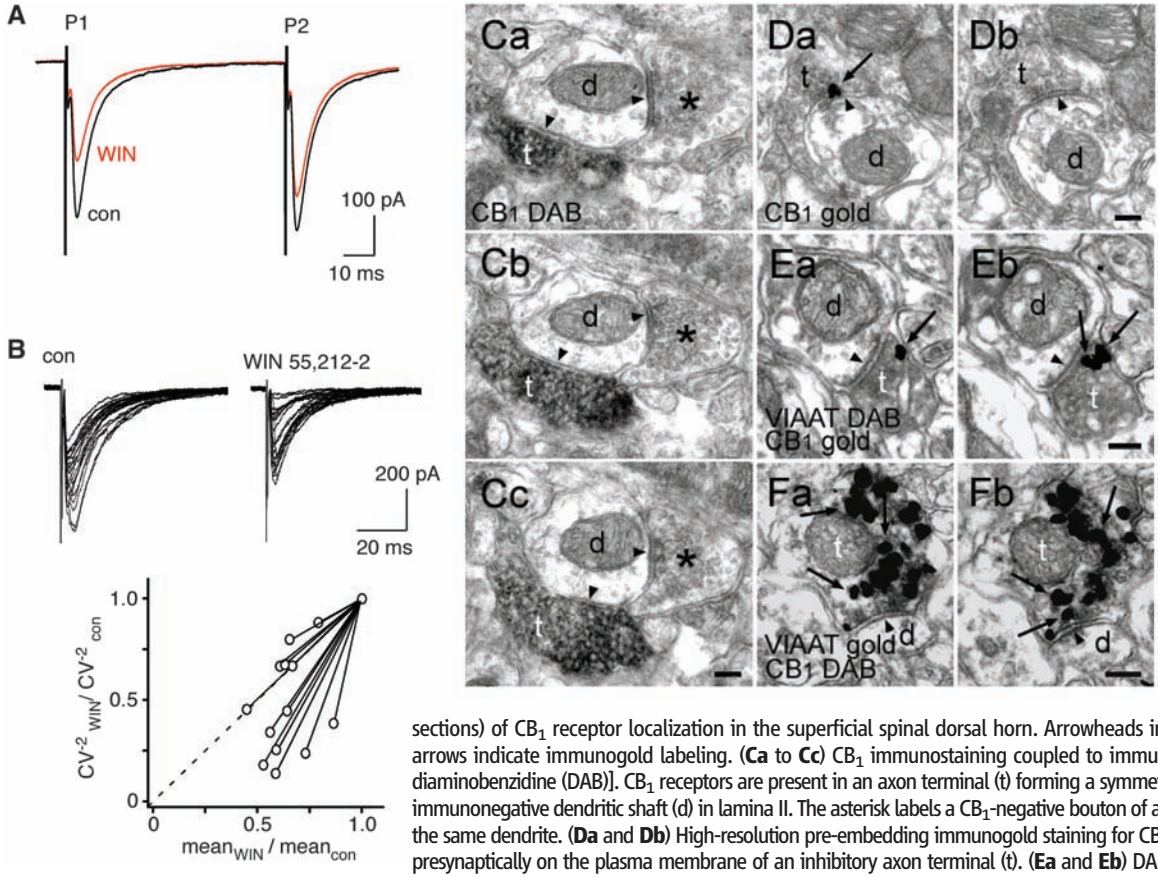

Fig. 2. Inhibition of glycinergic and GABAergic synaptic transmission via presynaptic CB_1 receptors. (**A**) Paired pulse experiments. Current traces of two consecutive glycinergic IPSCs (P1 and P2) under control conditions (black) and in the presence of 3 μM WIN 55,212-2 (red) are shown. (**B**) Variation analysis. Top panel: Individual traces of glycinergic IPSCs recorded under control conditions and in the presence of WIN 55,212-2 (3 μM). Bottom panel: Changes in the CV in 13 cells are plotted versus changes in the mean amplitude induced by WIN 55,212-2. (**C** to **F**) Electron microscopic analysis (**a** to **c** and **a** and **b** are serial sections) of CB_1 receptor localization in the superficial spinal dorsal horn. Arrowheads indicate symmetric synapses; arrows indicate immunogold labeling. (**Ca** to **Cc**) CB_1 immunostaining coupled to immunoperoxidase reaction [3,3′-diaminobenzidine (DAB)]. CB_1 receptors are present in an axon terminal (t) forming a symmetric (inhibitory) synapse on an immunonegative dendritic shaft (d) in lamina II. The asterisk labels a CB_1-negative bouton of another symmetric synapse on the same dendrite. (**Da** and **Db**) High-resolution pre-embedding immunogold staining for CB_1. The CB_1 receptor is located presynaptically on the plasma membrane of an inhibitory axon terminal (t). (**Ea** and **Eb**) DAB staining for VIAAT and pre-embedding immunogold labeling for CB_1. CB_1 cannabinoid receptors (indicated by arrows) are on an inhibitory (VIAAT-positive) axon terminal (t). In this reaction, silver intensification results in weaker electron density of the DAB precipitate. (**Fa** and **Fb**) Immunoperoxidase staining for CB_1 combined with pre-embedding immunogold labeling for VIAAT demonstrates colocalization of the two proteins. Similar results were obtained in four animals. Scale bar, 0.1 μm.

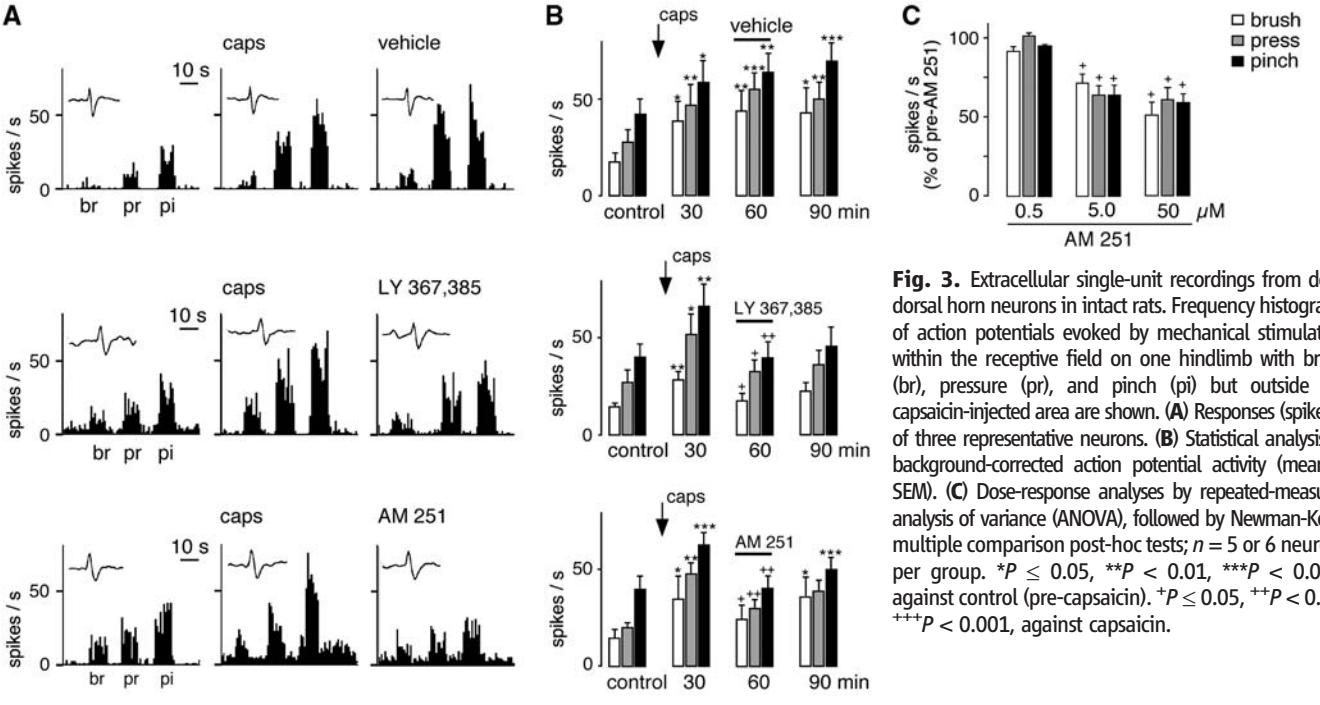

Fig. 3. Extracellular single-unit recordings from deep dorsal horn neurons in intact rats. Frequency histograms of action potentials evoked by mechanical stimulation within the receptive field on one hindlimb with brush (br), pressure (pr), and pinch (pi) but outside the capsaicin-injected area are shown. (**A**) Responses (spikes/s) of three representative neurons. (**B**) Statistical analysis of background-corrected action potential activity (mean ± SEM). (**C**) Dose-response analyses by repeated-measures analysis of variance (ANOVA), followed by Newman-Keuls multiple comparison post-hoc tests; n = 5 or 6 neurons per group. $^{*}P \leq 0.05$, $^{**}P < 0.01$, $^{***}P < 0.001$, against control (pre-capsaicin). $^{+}P \leq 0.05$, $^{++}P < 0.01$, $^{+++}P < 0.001$, against capsaicin.

ished release of GABA and glycine from inhibitory nerve terminals. In paired pulse experiments, WIN 55,212-2 (3 μM) increased the amplitude ratio of two consecutive IPSCs, 70 ms apart, from 1.14 ± 0.07 to 1.61 ± 0.15 (n = 5 neurons, $P < 0.05$, paired Student's t test) (Fig. 2A). Accordingly, the coefficient of variation [CV = $(SD^2/mean^2)^{1/2}$] of IPSC amplitudes (*15*) increased from 0.190 ± 0.012 under control conditions to 0.306 ± 0.031 in the presence of WIN 55,212-2, again indicative of a presynaptic action (n = 13 neurons, $P < 0.01$, paired Student's t test) (Fig. 2B). We directly demonstrated the presence of CB_1 receptors on the presynaptic terminals of inhibitory mouse superficial dorsal horn neurons by electron microscopy (EM) (Fig. 2, C to F). Peroxidase-based and immunogold labeling of CB_1 receptors and high-resolution EM unequivocally showed the presence of CB_1 receptors on presynaptic terminals of symmetrical (inhibitory) synapses (Fig. 2, C and D) and the colocalization of CB_1 with the vesicular inhibitory amino acid transporter (VIAAT) (Fig. 2, E and F), a marker of inhibitory axon terminals (*16*).

We next studied the role of endocannabinoids in secondary hyperalgesia in intact rats and performed in vivo extracellular single-unit recordings (*10*) from neurons with a wide dynamic range (that is, neurons responding to both noxious and innocuous stimulation) with receptive fields in the hindpaw and located in the deep lumbar dorsal horn (Fig. 3). Intracutaneous injection of capsaicin (200 μg) into the receptive field of the recorded neuron led to a robust increase in action potential firing in response to mechanical stimulation in an area surrounding the capsaicin injection site, akin to secondary hyperalgesia and allodynia. This increase was reversed by local spinal application not only of the mGluR1 antagonist LY 367,385 (10 μM, n = 5 neurons) but also of the CB_1 receptor blocker AM 251 (5 and 50 μM, n = 5 or 6 neurons).

In mice, we tested the effects of pharmacological and genetic manipulation of the endocannabinoid system on capsaicin-induced secondary hyperalgesia (Fig. 4). Subcutaneous injection of capsaicin (30 μg) into one hindpaw of wild-type mice led to a reduction in paw withdrawal thresholds in response to mechanical stimulation with dynamic von Frey filaments from 2.85 ± 0.04 g under control conditions to 0.53 ± 0.10 g (mean ± SEM, n = 6 mice) at 2 hours after capsaicin injection (*10*). Intrathecal injection (injection into the lumbar spinal canal) of the mGluR1 antagonist LY 367,385 (1.0 nmol per mouse) 2 hours after capsaicin reduced mechanical sensitization by 64.9 ± 2.9% (n = 6 mice) (*17*). Consistent with the role of CB_1 receptors in synaptic disinhibition, intrathecal AM 251 (0.5 nmol) reversed mechanical sensitization by 71.2 ± 9.0% (n = 6 mice). Accordingly, inhibition of endocannabinoid degradation with URB 597 or of endocannabinoid reuptake with UCM 707 (each 1.0 nmol) (*18*) prolonged secondary hyperalgesia (Fig. 4A). In naïve mice, all five compounds exerted only minor effects on mechanical sensitivity (fig. S4).

Global $CB_1^{-/-}$ mice and *ptf1a*-$CB_1^{-/-}$ mice were protected from capsaicin-induced mechanical sensitization. In contrast, mice devoid of CB_1 receptors only in primary afferent nociceptors (*sns*-$CB_1^{-/-}$ mice) (*19*) developed normal secondary hyperalgesia (Fig. 4B), indicating that the CB_1 receptors on inhibitory dorsal horn neurons, and not those on primary nociceptors, mediated capsaicin-induced secondary hyperalgesia. The unchanged responses of *sns*-$CB_1^{-/-}$ mice also indicate that possible direct interactions of CB_1 receptors with TRPV1 channels (*20*, *21*) expressed on the spinal terminals of primary nociceptors were not involved.

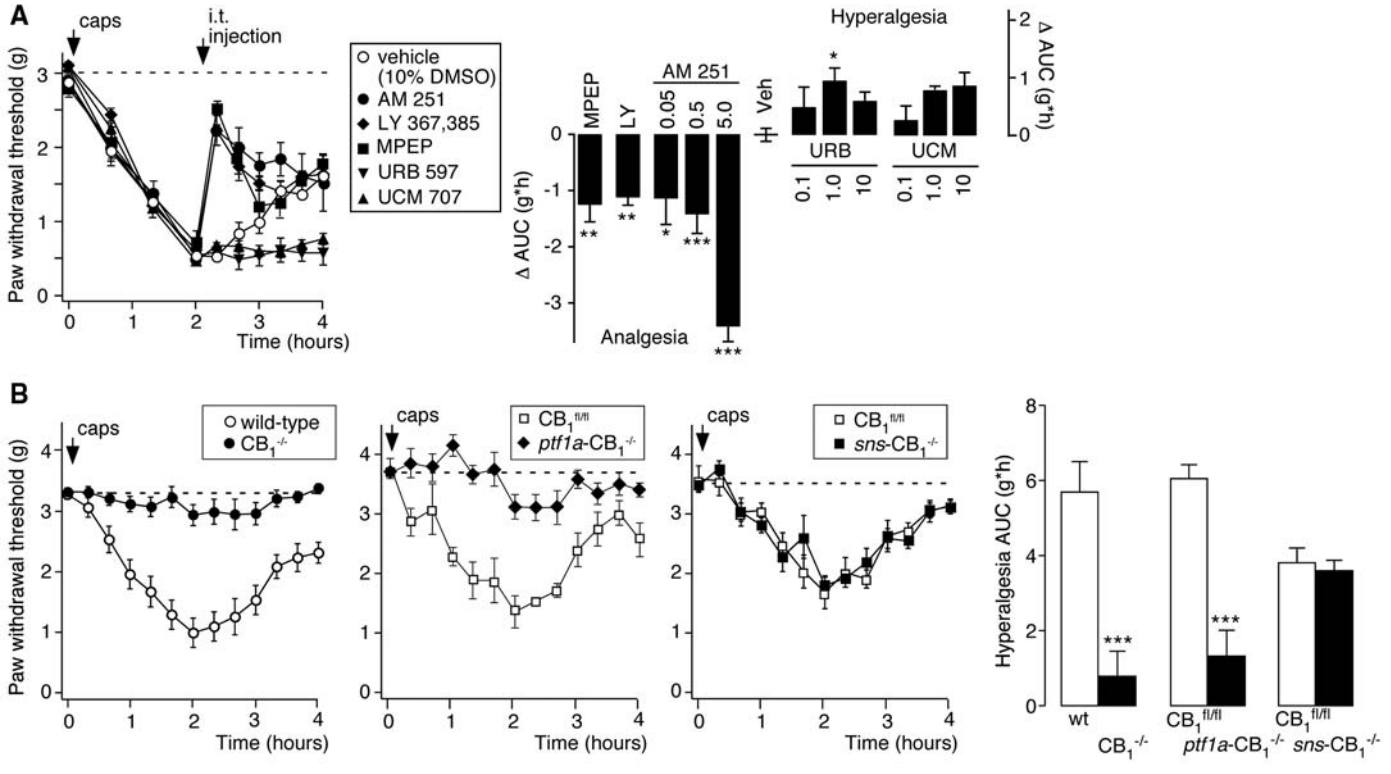

Fig. 4. Effects of pharmacological and genetic manipulations of the endocannabinoid system on capsaicin-induced mechanical hyperalgesia in mice. (**A**) Mechanical paw withdrawal thresholds (mean ± SEM) were determined with dynamic von Frey filaments at 20-min intervals for 2 hours after capsaicin injection into the left hindpaw and for another 2 hours after intrathecal injections of vehicle (10% dimethyl sulfoxide), AM 251 (0.5 nmol per mouse), URB 597 (1.0 nmol), UCM 707 (1.0 nmol), LY 367,385 (1.0 nmol), or MPEP (150 nmol). Left panel: Time course (mean ± SEM). Right panel: Treatment-induced changes in hyperalgesia. Areas under the curve (AUC) were integrated over time from 2 to 4 hours after capsaicin injection. The time course of sensitization in wild-type mice treated with intrathecal vehicle is the same as in wild-type mice that did not receive intrathecal injections (B). n = 5 or 6 mice per group; for statistical analyses, three groups of vehicle-injected mice were pooled. Analyses were by one-way ANOVA followed by Dunnett's post-hoc test $F(11,74) = 21.18$; $^*P \leq 0.05$, $^{**}P < 0.01$, $^{***}P < 0.001$. (**B**) Capsaicin-induced secondary hyperalgesia in wild-type mice versus $CB_1^{-/-}$ mice (n = 9 mice per group) and in *ptf1a*-$CB_1^{-/-}$ mice (n = 7 and 11 mice per group) and *sns*-$CB_1^{-/-}$ mice versus mice carrying a CB_1 receptor gene flanked by two *loxP* sites ($CB_1^{fl/fl}$ mice) (n = 5 mice per group). Left: Time course. Right: AUC (0 to 4 hours after capsaicin injection). $^{***}P < 0.001$, unpaired Student's t test.

Mechanical sensitization could also be evoked by intrathecal injection of the CB_1/CB_2 agonist CP 55,940 (fig. S5). Intrathecal CP 55,940 (10 nmol) significantly decreased the thresholds of mechanical stimulation with von Frey filaments in wild-type ($CB_1^{fl/fl}$) and *sns*-$CB_1^{-/-}$ mice and rendered both types of mice extremely sensitive to touch. In both tests, mechanical sensitization by CP 55,940 was absent in global $CB_1^{-/-}$ mice. The pronociceptive effects of endocannabinoids suggested here are specific for C-fiber–mediated, activity-dependent hyperalgesia. In models of mild inflammatory pain (produced by subcutaneous injection of zymosan A) (*10*) and neuropathic pain (produced by chronic constriction injury) (*10*), $CB_1^{-/-}$ mice behaved normally (fig. S6, A and B). AM 251 had only negligible effects (fig. S6, C and D), whereas CP 55,940 exerted anti-hyperalgesic actions in these models (fig. S6, E and F). Both of these models also involve spinal disinhibitory processes, but the underlying mechanisms are most likely different and involve the spinal release of pronociceptive prostaglandin E_2 (*22*) and changes in the transmembrane chloride gradient (*23*).

Finally, we tested the effect of CB_1 receptor blockade on C-fiber–induced secondary hyperalgesia and allodynia in human volunteers (fig. S7). Secondary hyperalgesia was induced by intracutaneous electrical stimulation at C-fiber strength (2 Hz, 15 to 100 mA) of a small skin area of the left forearm (*10*). In the first session, the intensity of electrical stimulation was adjusted to yield a value of 6 on a numeric rating scale ranging from 0, no pain, to 10, maximum imaginable pain, and pain ratings and the sizes of hyperalgesic skin areas surrounding the site of electrical stimulation were determined for 100 min at regular intervals. In a second session, 28 days later, the volunteers were tested again after a 10-day treatment with either placebo or rimonabant (20 mg/day, aken rally), a CB_1 receptor antagonist/inverse agonist closely related to AM 251. Rimonabant treatment had no effect on acute pain ratings induced by electrical stimulation (–2.0 ± 5.7%, $n = 8$ volunteers per group) but decreased the sizes of hyperalgesic and allodynic skin areas to 53.7 ± 5.2 and 57.4 ± 5.0%, respectively.

The contribution of endocannabinoids to activity-dependent pain sensitization, which we propose here, builds on a model of secondary hyperalgesia and allodynia (fig. S8), in which normally pain-specific dorsal horn neurons receive not only monosynaptic input from C-fiber nociceptors but also polysynaptic input from non-nociceptive fibers (*24*). The suprathreshold activation of these neurons by such non-nociceptive input is normally prevented by the activity of dorsal horn inhibitory interneurons. The present study shows that intense glutamatergic input from C-fiber nociceptors diminishes this inhibitory control through endocannabinoids acting at CB_1 receptors located on dorsal horn inhibitory interneurons. Our findings thus attribute to endocannabinoids an unexpected role in dorsal horn neuronal circuits as mediators of spinal activity–dependent pain sensitization. They are also an example of a distinctive phenotype of mice lacking CB_1 receptors specifically in inhibitory interneurons, whereas most previously reported phenotypes of global CB_1 receptor–deficient mice could be ascribed to the lack of CB_1 receptors on glutamatergic neurons (*25*).

References and Notes

1. R. Meyer, M. Ringkamp, J. Campbell, S. Raja, in *Textbook of Pain*, S. B. McMahon, M. Koltzenburg, Eds. (Elsevier, Churchill Livingstone, 2006), pp. 3–34.
2. L. Sivilotti, C. J. Woolf, *J. Neurophysiol.* **72**, 169 (1994).
3. T. L. Yaksh, *Pain* **37**, 111 (1989).
4. R. D. Treede, W. Magerl, *Prog. Brain Res.* **129**, 331 (2000).
5. M. Kano, T. Ohno-Shosaku, Y. Hashimotodani, M. Uchigashima, M. Watanabe, *Physiol. Rev.* **89**, 309 (2009).
6. V. Chevaleyre, K. A. Takahashi, P. E. Castillo, *Annu. Rev. Neurosci.* **29**, 37 (2006).
7. W. P. Farquhar-Smith *et al.*, *Mol. Cell. Neurosci.* **15**, 510 (2000).
8. P. Pacher, S. Batkai, G. Kunos, *Pharmacol. Rev.* **58**, 389 (2006).
9. V. Di Marzo, *Nat. Rev. Drug Discov.* **7**, 438 (2008).
10. Materials and methods are available as supporting material on *Science* Online.
11. G. Marsicano *et al.*, *Nature* **418**, 530 (2002).
12. S. M. Glasgow, R. M. Henke, R. J. Macdonald, C. V. Wright, J. E. Johnson, *Development* **132**, 5461 (2005).
13. E. A. Jennings, C. W. Vaughan, M. J. Christie, *J. Physiol.* **534**, 805 (2001).
14. H. U. Zeilhofer *et al.*, *J. Comp. Neurol.* **482**, 123 (2005).
15. R. Malinow, R. W. Tsien, *Nature* **346**, 177 (1990).
16. F. A. Chaudhry *et al.*, *J. Neurosci.* **18**, 9733 (1998).
17. V. Neugebauer, P. S. Chen, W. D. Willis, *J. Neurophysiol.* **82**, 272 (1999).
18. D. Piomelli, *Nat. Rev. Neurosci.* **4**, 873 (2003).
19. N. Agarwal *et al.*, *Nat. Neurosci.* **10**, 870 (2007).
20. B. Fioravanti *et al.*, *J. Neurosci.* **28**, 11593 (2008).
21. M. Maccarrone *et al.*, *Nat. Neurosci.* **11**, 152 (2008).
22. R. J. Harvey *et al.*, *Science* **304**, 884 (2004).
23. J. A. Coull *et al.*, *Nature* **424**, 938 (2003).
24. C. Torsney, A. B. MacDermott, *J. Neurosci.* **26**, 1833 (2006).
25. K. Monory *et al.*, *PLoS Biol.* **5**, e269 (2007).

26. This research was supported in part by grants from the Schweizerischer National Fonds to H.U.Z. (3100A0-116064/1), from the Deutsche Forschungsgemeinschaft to W.K. (KO 1878/2-2) and H.U.Z. (ZE 377/8-2), from NIH (NS38261 and NS11255) to V.N., from the European Union (LSHM-CT-2004-005166) to T.F.F., and from the OTKA (F046407) and ETT (561/2006) to I.K. A.J.P.A. was supported partly by scholarships from the German DAAD and the Venezuelan FONACIT for graduate study at IVIC. I.K. was supported by a János Bolyai scholarship. The authors thank R. Kuner and C. V. Wright for providing *sns*-cre and *ptf1a*-cre mice, respectively; J.-M. Fritschy, H. Handwerker, H. Möhler, and M. Schmelz for critical reading of the manuscript; T. Müller for very valuable suggestions; and I. Camenisch and L. Scheurer for genotyping of the mice.

Supporting Online Material

www.sciencemag.org/cgi/content/full/325/5941/760/DC1
Materials and Methods
Figs. S1 to S8
Table S1
References

4 February 2009; accepted 24 June 2009
10.1126/science.1171870

An Alternative DNA Structure Is Necessary for Pilin Antigenic Variation in *Neisseria gonorrhoeae*

Laty A. Cahoon and H. Steven Seifert*

Pathogens can use DNA recombination to promote antigenic variation (Av) of surface structures to avoid immune detection. We identified a cis-acting DNA sequence near the antigenically variable pilin locus of the human pathogen, *Neisseria gonorrhoeae*. This 16–base pair guanine (G)–rich sequence was required for pilin Av and formed a guanine quartet (G4) structure in vitro. Individual mutations that disrupted the structure also blocked pilin Av and prevented nicks required for recombination from occurring within the G4 region. A compound that binds and stabilizes G4 structures also inhibited pilin Av and prevented nicks from occurring on the G-rich strand. This site constitutes a recombination initiation sequence/structure that directs gene conversion to a specific chromosomal locus.

DNA recombination is a process that is shared by all DNA-carrying organisms and used for a variety of cellular processes, including DNA repair, genetic exchange, and meiotic chromosome segregation (*1*). Additionally, recombination mediates many high-frequency gene-diversification systems, including yeast mating-type switches, immunoglobin diversity, and pathogenesis-associated antigenic variation (Av) (*2*–*4*). Most recombination reactions occur at a low frequency, but several diversity-generating systems can enact programmed recombination reactions between specific loci at relatively high frequencies (*2*, *3*, *5*, *6*).

Neisseria gonorrhoeae is the sole causative agent of gonorrhea and has evolved three high-frequency, diversity-generation systems to avoid immune surveillance (*7*). This antigenic variability of gonococcal populations is one reason that natural immunity to re-infection has never been demonstrated and has prevented the development of an effective vaccine. One of these Av systems is mediated by high-frequency gene-conversion events between one of many silent pilin loci and the single expressed pilin locus,

Northwestern University Feinberg School of Medicine, 303 East Chicago Avenue, Chicago, IL 60611, USA.

*To whom correspondence should be addressed. E-mail: h-seifert@northwestern.edu